https://doi.org/10.5194/cp-2021-163
Preprint. Discussion started: 29 November 2021

Climate of the Past Discussions
Open Access
EGU

Calendar effects on surface air temperature and precipitation based on model-ensemble equilibrium and transient simulations from PMIP4 and PACMEDY

Xiaoxu Shi[1], Martin Werner[1], Carolin Krug[1,2], Chris M. Brierley[3], Anni Zhao[3], Endurance Igbinosa[1,2], Pascale Braconnot[4], Esther Brady[5], Jian Cao[6], Roberta D'Agostino[7], Johann Jungclaus[7], Xingxing Liu[8], Bette Otto-Bliesner[5], Dmitry Sidorenko[1], Robert Tomas[5], Evgeny M. Volodin[9], Hu Yang[1], Qiong Zhang[10], Weipeng Zheng[11], and Gerrit Lohmann[1,2]

[1]Alfred Wegener Institute, Helmholtz Center for Polar and Marine Research, Bremerhaven, Germany
[2]Bremen University, Bremen, Germany
[3]Dept. of Geography, University College London, London, UK
[4]Laboratoire des Sciences du Climat et de l'Environnement-IPSL, Unité Mixte CEA-CNRS-UVSQ, Université Paris-Saclay, Orme des Merisiers, Gif-sur-Yvette, France
[5]Climate and Global Dynamics Laboratory, National Center for Atmospheric Research (NCAR), Boulder, CO 80305, USA
[6]School of Atmospheric Sciences, Nanjing University of Information Science & Technology, Nanjing, 210044, China
[7]Max Planck Institute for Meteorology, Hamburg, Germany
[8]State Key Laboratory of Loess and Quaternary Geology, Institute of Earth Environment, Chinese Academy of Sciences, Xi'an, 710061, China
[9]Marchuk Institute of Numerical Mathematics, Russian Academy of Sciences, ul. Gubkina 8, Moscow, 119333, Russia
[10]Department of Physical Geography and Bolin Centre for Climate Research, Stockholm University, 10691, Stockholm, Sweden
[11]LASG, Institute of Atmospheric Physics, Chinese Academy of Sciences, Beijing, 100029, China

Correspondence: Xiaoxu Shi (xshi@awi.de)

Abstract. Numerical modelling enables a comprehensive understanding not only of the Earth's system today, but also of the past. To date, a significant amount of time and effort has been devoted to paleoclimate modeling and analysis, which involves the latest and most advanced Paleoclimate Modelling Intercomparison Project phase 4 (PMIP4). The definition of seasonality, which is influenced by slow variations in the Earth's orbital parameters, plays a key role in determining the calculated seasonal cycle of the climate. In contrast to the classical calendar used today, where the lengths of the months and seasons are fixed, the angular calendar calculates the lengths of the months and seasons according to a fixed number of degrees along the Earth's orbit. When comparing simulation results for different time intervals, it is essential to account for the angular calendar to ensure that the data for comparison is from the same position along the Earth's orbit. Most models use the classical "fixed-length" calendar, which can lead to strong distortions of the monthly and seasonal values, especially for the climate of the past. Here, by analyzing daily outputs from multiple PMIP4 model simulations, we examine calendar effects on surface air temperature and precipitation under mid-Holocene, last interglacial, and pre-industrial climate conditions. We conclude that: (a) The largest cooling bias occurs in autumn when the classical calendar is applied for the mid-Holocene and last interglacial. (b) The sign of the temperature anomalies between the Last Interglacial and pre-industrial in boreal autumn can be reversed after the switch from classical to angular calendar, particularly over the Northern Hemisphere continents. (c) Precipitation over West Africa is

https://doi.org/10.5194/cp-2021-163
Preprint. Discussion started: 29 November 2021

Climate of the Past Discussions

overestimated in boreal summer and underestimated in boreal autumn when the "fixed-length" seasonal cycle is applied. (d) Finally, correcting the calendar based on the monthly model results can reduce the biases to a large extent, but not completely eliminate them. In addition, we examine the calendar effects in 3 transient simulations for 6-0 ka by AWI-ESM, MPI-ESM, and IPSL. We find significant discrepancies between adjusted and unadjusted temperature values over ice-free continents for both hemispheres in boreal autumn. While for other seasons the deviations are relatively small. A drying bias can be found in the summer monsoon precipitation in Africa (in the "fixed-length" calendar), whereby the magnitude of bias becomes smaller over time. Overall, our study underlines the importance of the application of calendar transformation in the analysis of climate simulations. Neglecting the calendar effects could lead to a profound artificial distortion of the calculated seasonal cycle of surface air temperature and precipitation. One important fact to be noted here is that the discrepancy in seasonality under different calendars is an analysis bias and is highly depends on the choice of the reference position/date (usually the vernal equinox, which is set to 31th March) on the Earth's ellipse around the sun. Different model groups may apply different reference dates, so ensuring a consistent reference date and seasonal definition is key when we compare results across multiple models.

1 Introduction

Long-term fluctuations exist in the earth's orbital elements that affect the amount of solar radiation received by our planet (Berger, 1977). There are three parameters controlling the motion of the Earth: eccentricity, obliquity and precession. The shape of the Earth's orbit varies over time from nearly circular with a small eccentricity of 0.0034 to slightly elliptical (large eccentricity of 0.058) with a periodicity of about 100,000 years. When the eccentricity is large, there is a big difference in the incoming solar radiation between periods of perihelion and aphelion, while at a small eccentricity when the orbit is more circular this difference is less pronounced. Earth's orbital eccentricity is 0.0167, 0.0189, and 0.0397 in the present, mid-Holocene and Last Interglacial respectively. The seasons are caused by the tilt of the Earth's axis, which is called obliquity. Boreal summer occurs when the Earth's North Pole is tilted toward the sun, and vice versa when boreal winter prevails. Earth's axial obliquity oscillates between 22.1 and 24.5 degrees with a period of 41,000 years. A high obliquity results in stronger seasonal cycles than a low obliquity does. At the same time, the Earth wobbles around its axis (precession), such movement fluctuates with a period of 19,000 to 23,000 years. Precession determines the beginning of each season relative to Earth's orbit and therefore has a major impact on the seasonal pattern of solar radiation. Understanding the role of the three elements of Earth's orbit can help us better examine and interpret past climates from seasonal to millennial time scales.

Numerical modeling of the past climate, which is very different from today, can in many aspects improve our understanding of the underlying mechanisms of the Earth's system and help us better predict the future climate. The Paleoclimate Model Intercomparison Project (PMIP) brings together a bunch of model groups, providing the ability to synchronize results from different models (Kageyama et al., 2018, 2021a).

https://doi.org/10.5194/cp-2021-163
Preprint. Discussion started: 29 November 2021

Climate of the Past Discussions

Two interglacial episodes, i.e., the mid-Holocene (MH, 6 ka, B.P.) and the Last Interglacial (LIG, 127 ka B.P.), are particularly the focus of PMIP (Otto-Bliesner et al., 2017), as they are the two most recent warm periods in geological history that have great potential to resemble future scenarios under global warming. So far, there are a variety of previous studies aiming to examine the simulated climate of mid-Holocene and Last Interglacial. Due to the Earth's orbital parameter anomalies with respect to the present, the MH and LIG receive more insolation in summer and less in winter, leading to enhanced seasonal cycles in the two time periods (Kukla et al., 2002; Shi and Lohmann, 2016; Shi et al., 2020; Zhang et al., 2021; Kageyama et al., 2021b). Such effect is much more profound in the LIG than in the MH, especially for the Northern Hemisphere (Lunt et al., 2013; Pfeiffer and Lohmann, 2016). Climate models identified a northward shift of the Intertropical Convergence Zone (ITCZ) during the two periods, accompanied by a northward displacement of the Northern Hemisphere monsoon domains (Jiang et al., 2015; Braconnot et al., 2007; Nikolova et al., 2012; Fischer and Jungclaus, 2010). The precession of the MH and LIG, which determines the length of each season, was also different from today. Following the orbital definition of seasons, this results in a calendar (hereafter referred to as angular calendar) that is different from today's calendar (hereafter referred to as fixed-length or classical calendar). It has been pointed out in Joussaume and Braconnot (1997) that significant biases occur when we apply today's fixed-length calendar to the MH and LIG seasonal cycles. Therefore, it is important to consider the orbital configuration when defining seasonal cycles for past climate. However, the effect of calendar in most recent paleoclimate simulations has not been investigated. A recent study by Bartlein and Shafer (2019) examined the "pure" responses of temperature and precipitation to calendar conversion; this was accomplished by applying angular calendars of 6, 97, 116 and 127 ka in a modern climate state. Our present study differs from Bartlein and Shafer (2019) in the following aspects: 1. We use daily data instead of monthly data, so a more accurate result is guaranteed. 2. We perform calendar correction for pre-industrial as well, as today's Gregorian calendar is not an angular one. It should be noted that in most previous studies today's calendar has been left unchanged (Joussaume and Braconnot, 1997; Bartlein and Shafer, 2019). 3. Instead of investigating the "pure" calendar effect, we perform calendar adjustment based on actual paleo-experiments so that the boundary conditions also play a role.

In the present study, we use the PMIP4 dataset to investigate the calendar effect on the simulated surface air temperatures and precipitation under MH and LIG boundary conditions. The structure of the paper is as follows: In Section 2, we describe the method for defining an angular calendar based on the Earth's orbital parameters and provide detailed information on the data we used. Section 3 presents the results. We discuss and conclude in Section 4.

2 Methodology

2.1 Calendar correction

In order to appropriately compare the seasonal climate between different time periods resonating with the respective orbital configuration, the seasonality should be calculated according to the position of the Earth along its orbit. First, we define the true anomaly θ as the angle between the axis of the perihelion and the actual position of the earth. Note that the term "anomaly", standing for "angle", is used in astronomy to describe planetary positions. We then define a month (season) as a 30 (90 degree)

https://doi.org/10.5194/cp-2021-163
Preprint. Discussion started: 29 November 2021


Climate of the Past Discussions
Open Access
EGU

increment of the true anomaly, integrated from a fixed starting point. The vernal equinox (VE) of the Northern Hemisphere is set on March 21 at noon. In the following, we compute the length of a month (season) by calculating how much time the Earth needs to move from the respective starting point to the endpoint. For this purpose, we derive the relation between the true anomaly of any given time and the time elapsed since the Earth passes perihelion.

We define the mean anomaly M as the angle between the perihelion and Earth's position based on the assumption that the orbit describes a perfect circle with the sun at the center by:

$$M = \frac{2\pi}{T} \cdot t_p \tag{1}$$

Here, t_p denotes the time elapsed since Earth passes the perihelion and T is the orbital period (i.e., one year). Taking into account the orbit's eccentricity ϵ, we define the eccentric anomaly E via:

$$E - \epsilon \cdot \sin(E) = M \tag{2}$$

Equation (2) can be solved with the application of Newton's method. For more detailed information we refer to Danby and Burkardt (1983). The true anomaly θ is then defined by:

$$\theta = 2 \cdot \arctan\left(\sqrt{\frac{1+\epsilon}{1-\epsilon}} \cdot \tan\left(\frac{E}{2}\right)\right) \tag{3}$$

The above equations implicitly relates t_p to θ.

The calendar correction method can only be suitably applied on daily data. If only monthly data is available, an alternative option is to reconstruct the daily time series in a way that original monthly mean averages are preserved, then to perform calendar conversion based on the reconstructed daily time series. The mean preserving algorithm is presented in Rymes and Myers (2001).

Note that, although the VE is set to March 21st, we define seasons as typically done in paleoclimate modelling by applying the "meteorological" definition and averaging over the respective months in order to compare the angular seasonal means with the classical seasonal means.

2.2 Data

We collect the PMIP4 models which provide daily outputs of surface air temperature and precipitation for equilibrium simulations of pre-industrial, mid-Holocene and Last Interglacial. There are 9 models that meet the requirement, and we list the detailed information of those models in Table 1.

Besides equilibrium simulations, we also use the monthly surface air temperature and precipitation from 3 transient simulations for the past 6,000 years, based on the Earth system models AWI-ESM, MPI-ESM, and IPSL. Using AWI-ESM, we have conducted one 6-0 ka transient experiment with dynamic vegetation, by applying the boundary conditions of the past

https://doi.org/10.5194/cp-2021-163
Preprint. Discussion started: 29 November 2021

Climate of the Past Discussions
Open Access
EGU

Table 1. List of PMIP4 model data used in the present study.

Name	Institution	Reference	Notes
AWI-ESM-1-1-LR	AWI	Sidorenko et al. (2015); Rackow et al. (2018)	Dynamic vegetation
AWI-ESM-2-1-LR	AWI	Sidorenko et al. (2019)	Dynamic vegetation
CESM2	NCAR	Gettelman et al. (2019)	Potential Natural Land Cover
EC-Earth3-LR	Stockholm University		Prescribed vegetation and aerosols
FGOALS-f3-L	IAP-CAS	He et al. (2019)	-
FGOALS-g3	IAP-CAS	Li et al. (2020)	-
INM-CM4-8	INM RAS	Volodin et al. (2018)	Prescribed vegetation, simulated aerosols
IPSL-CM6A-LR	IPSL	Lurton et al. (2020)	Prescribed vegetation, interactive phenology, prescribed PI aerosols
NESM3	NUIST	Cao et al. (2018)	-

6,000 years with the last year representing 1950 CE. Orbital parameters are calculated according to Berger (1977), and the greenhouse gases are taken from ice-core records and from recent measurements of firn air and atmospheric samples (Köhler et al., 2017). The transient simulation performed by MPI-ESM spans the period from 6000 BP until 1850 CE. The model is forced by prescribed orbitally-induced variations in the insolation following Berger (1977). CO2, N2O and CH4 forcings stem from ice-core reconstructions (Brovkin et al., 2019). The model accounts for dynamic vegetation changes in the land-surface model JSBACH. A more detailed description of the boundary conditions and the forcing of the transient simulation are given in Bader et al. (2020). The IPSL transient simulation was initialized from a 1,000-year mid-Holocene spin-up run. The Earth's orbital parameters are derived from Berger (1977), the concentrations of the trace gases (CO2, CH4 and N2O) are set based on reconstruction from ice core data (Joos and Spahni, 2008), and the vegetation was calculated interactively within the model. More detailed information about the IPSL transient simulation can be found in Braconnot et al. (2019).

3 Results

3.1 Climate responses to the MH and LIG boundary conditions under classical calendar

Owing to the altered orbital parameters, the MH receives more (less) incoming solar radiation over the Northern Hemisphere during boreal summer (winter) than present (Fig. S1a). As a consequence, the MH Northern Hemisphere experiences a cooling (up to -2 K) and warming (up to 2.5 K) in DJF and JJA respectively (Fig. S2a-b). For the annual average, our model ensemble reveals a general cooling (Fig. S2c) over Northern Hemisphere, which seems to be inconsistent with the increased insolation forcing. This phenomenon can be explained by the decreased concentration of greenhouse gases in the MH as compared to

https://doi.org/10.5194/cp-2021-163
Preprint. Discussion started: 29 November 2021


Climate of the Past Discussions

present-day condition, which leads to an effective radiative forcing of about -0.3 W/m2, as estimated by Otto-Bliesner et al. (2017).

Regarding the Southern Hemisphere we observe a general cooling in DJF (Fig. S2a), dominated by the decreased insolation in January and February (Fig. S1a). The warming across the Southern Ocean is due to a delayed effect of the increased solar energy in SON. Moreover, the models present a robust cooling over most regions of Southern Hemisphere in JJA, which is mainly led by the reduction in greenhouse gases as the difference in the incomming solar radiation between the MH and PI is negligible.

The changes in surface air temperature in the LIG with respect to the PI, as shown in Fig. S2d-f, are much more pronounced than that between the MH and the PI. The most intriguing feature is an enhancement in seasonality during the LIG, with a DJF cooling being up to -5 K (over North Africa and South Asia), as well as a JJA warming (more then 5 K) at the North America and Eurasia. This is mostly contributed by the corresponding anomalies in solar insolation (Fig. S1c). In addition, the model-ensemble produces a cooling over Sahal region as a response to the intensification in monsoonal rainfall. For the Southern Hemisphere, the subtropical continents also experience a DJF cooling and JJA warming (more then 2 K) as responses to the altered incoming solar radiation. Such feature is robust across the models.

The summer monsoon precipitation is shown to be enhanced over the Northern Hemisphere monsoon domains, in both MH and LIG as compared to modern condition (Fig. S2g-l), driven by the changes in seasonal insolation and the northward displacement of the Inter Tropical Convergence Zone (ITCZ). The monsoon domain at northern Africa, as well as South Asia, expands significantly in the LIG in relative to PI, associated with a stronger land-sea thermal contrast, and an intensification of moisture transport during monsoon seasons. Our results in terms of the responses of the surface air temperature and precipitation to the MH and LIG boundary conditions are in good agreement with the results from the full PMIP4 ensemble as described in Brierley et al. (2020) and Otto-Bliesner et al. (2021).

3.2 Shifts in months/seasons between classical and angular calendars

The calculated duration of the angular months and seasons is shown in Table 2. For PI, the shifts in the beginning of most months between the classical and angular calendar are generally in the range of -1 to 2 days, with the exception of October with a 3-day shift. So for today the two approaches are similar. Since the orbital velocity of the Earth is greater today at perihelion than at aphelion, we have fewer days in winter and more days in summer. This is reflected both in the classical calendar (DJF: 90 days; JJA: 92 days) and in the angular calendar (DJF: 89 days; JJA: 93 days) for today. The shifts of months for MH are in the range of -2 to 3 days, and the largest shift occurs mainly in the boreal winter. In the MH, winter and spring are longer in the angular calendar than in the classical calendar, while summer and autumn are shorter. Due to the large difference in precession in the LIG compared to today, there are significant shifts in the beginning of the months between classical and angular calendars, especially in autumn (about -10 days). During the LIG, winter has 98 days when the angular calendar is used, which is much longer than summer (85 days).

https://doi.org/10.5194/cp-2021-163
Preprint. Discussion started: 29 November 2021

Climate of the Past Discussions
Open Access
EGU

Table 2. Starting and end date of Angular month in PI, MH and LIG, referencing to today's fixed-length calendar in a no-leap year. Note that today's calendar is not an angular calendar and should be corrected as well.

Month/Season	PI	MH	LIG
Jan.	02Jan.-30Jan.	29Dec.-28Jan.	26Dec.-27Jan.
Feb.	31Jan.-01Mar.	29Jan.-28Feb.	28Jan.-28Feb.
Mar.	02Mar.-31Mar.	01Mar.-31Mar.	01Mar.-31Mar.
Apr.	01Apr.-01May.	01Apr.-02May.	01Apr.-30Apr.
May.	02May.-01Jun.	03May.-02Jun.	01May.-29May.
Jun.	02Jun.-02Jul.	03Jun.-03Jul.	30May.-26Jun.
Jul.	03Jul.-02Aug.	04Jul.-02Aug.	27Jun.-24Jul.
Aug.	03Aug.-02Sep.	03Aug.-01Sep.	25Jul.-22Aug.
Sep.	03Sep.-03Oct.	02Sep.-30Sep.	23Aug.-20Sep.
Oct.	04Oct.-02Nov.	01Oct.-29Oct.	21Sep.-21Oct.
Nov.	03Nov.-02Dec.	30Oct.-28Nov.	22Oct.-22Nov.
Dec.	03Dec.-01Jan.	29Nov.-28Dec.	23Nov.-25Dec.
Winter	03Dec.-01Mar. (89)	29Nov.-28Feb. (92)	23Nov.-28Feb. (98)
Spring	02Mar.-01Jun. (92)	01Mar.-02Jun. (94)	01Mar.-29May. (90)
Summer	02Jun.-02Sep. (93)	03Jun.-01Sep. (91)	30May.-22Aug. (85)
Autumn	03Sep.-02Dec. (91)	02Sep.-28Nov. (88)	23Aug.-22Nov. (92)

3.3 Calendar effects in equilibrium simulations

Now we turn to examine the calendar effects on the seasonal cycle of surface air temperature. Fig. 1 depicts the differences in seasonal surface air temperature between angular and classical means. Positive/negative values indicate cooling/warming bias if fixed-length calendar is used to describe the seasonal cycle. We observe spatially-variable changes of surface air temperature in adjusted values as compared to unadjusted values. For the LIG, the most pronounced pattern is a warming over the Northern Hemisphere up to 5 K in boreal autumn (SON), as well as a cooling over the Southern Hemisphere especially the Antarctic continent (up to -3 K). This is explicable by the fact that the angular SON receives more/less insolation over Northern/Southern Hemisphere than the classical SON does (Fig. 2a, Fig. S1), in agreement with the earlier onset of those months. As the VE is fixed at March 21st, the calendar effect is expected to be relatively minor for boreal spring (MAM). Indeed, we find only slight increase (within 0.3 K) in the Northern Hemisphere surface air temperature in classical means as compared to angular means, and for the Southern Hemisphere the calendar-adjusted minus unadjusted values are in the range of -0.1 to 0 K, dominated by the pattern in May (Fig. S3). We are aware of that there is no difference between adjusted and unadjusted values in March and April, as no shift occurs in the beginning and duration of these two months (Table 2). In boreal winter (DJF), the most prominent calendar effects on LIG surface air temperature can be seen over Northern Hemisphere, with a warming up to 1.5 K, as well as the oceans of Southern Hemisphere which experiences a cooling up to -0.4 K. Such pattern is dominated by the

https://doi.org/10.5194/cp-2021-163
Preprint. Discussion started: 29 November 2021

Climate of the Past Discussions

temperature anomalies in December (Fig. S3). The warming signal over Antarctica (0-0.5 K) in DJF, is mainly determined by increased insolation during January and February. The conversion of the calendar produces a cooling (within -1 K) over Northern Hemisphere ocean and Southern Hemisphere continents (except Antarctic) in boreal summer (JJA), while for other regions, especially the Northern Hemisphere continents, we obtain positive anomalies in surface air temperature.

Compared to the LIG, the response of surface air temperature to calendar effect in the MH are less pronounced (Fig. 1). It reveals a dipole pattern in all seasons, with warming over the Northern Hemisphere and cooling over the Southern Hemisphere. One exception is the Antarctica warming in boreal winter, led by the increased insolation in January and February over Antarctica (Fig. 2b). Fig. S4 shows the adjusted minus non-adjusted temperatures for each month. No difference is found for March as for mid-Holocene the beginning and end of March in the angular calendar are the same as in the modern fixed-length calendar (Table 2). From April to June, the delay in the angular calendar leads to a positive insolation difference and therefore a warming over the Northern Hemisphere, while the opposite case is for the Southern Hemisphere. Similar patterns are observed for October to November, but is due to an advance in those months (the peak insolation happens in June). In general, we notice that the temperature anomalies on continents are in phase with the insolation changes, while the calendar effect on surface air temperature over the ocean is delayed.

For PI, the classical "fixed-length" calendar used at present is similar to today's angular calendar from January to June (Table 2), this leads to relatively minor changes in surface air temperature in boreal winter, spring and summer (Fig. 1i-k, Fig. S5) in angular mean values as compared to classical mean values. In boreal autumn, a dipole pattern of insolation anomaly is obvious (Fig. 2c): less (more) insolation is received at the top of the atmosphere over Northern (Southern) Hemisphere in adjusted SON than that in non-adjusted SON, consistent with the delay of boreal autumn in angular calendar as compared to classical calendar. Such a pattern favors cooling (up to -0.4 K) over the Northern Hemisphere and warming over the Southern Hemisphere during SON.

Knowing the pure calendar effect on the surface air temperature for respective time period, now we turn to investigate to what degree the temperature anomalies between paleo and pre-industrial can be affected by calendar conversion. As shown by Fig. 3, in boreal winter, spring, and summer, we observe similar patterns for both definitions of seasonal means. The insolation changes induced by changes in orbital parameters produce an enhanced seasonality in LIG as compared to PI, with colder winter and warmer summer, especially over Northern Hemisphere continents. However, with classical calendar applied, the DJF cooling over Northern Hemisphere is overestimated by up to 1 K. Whilst an underestimation in the MAM cooling happen over Northern Hemisphere, with a magnitude up to 1 K. For JJA, the bias in temperature anomaly, as calculated from classical means, is not uniform and has a clear land-sea contrast. Classical calendar tends to underestimate the JJA warming over Northern Hemisphere lands (by 1 K) and Southern Hemisphere oceans (0.2 K); while the warming over North Atlantic, North Pacific, as well as Southern Hemisphere continents are overestimated in classical calendar. The most prominent calendar effect can be seen in SON, as the temperature anomaly over Northern Hemisphere continents in SON flips its sign after switching from classical means to angular means, with the magnitude of the bias being as large as -5 K for classical means. Such artificial bias could be interpreted as climatic signals without the application of the adjusted calendar.

https://doi.org/10.5194/cp-2021-163
Preprint. Discussion started: 29 November 2021

Climate of the Past Discussions

For the temperature anomalies between MH and PI, the most significant bias introduced by the use of the classical calendar occurs in SON over Northern Hemisphere continents (more than 1 K), which appears to be colder in MH as compared to PI for classical means, and warmer for angular means. Moreover, the warming over Antarctica in MH relative to PI is overestimated in the classical calendar. From DJF through MAM, both calendars show a general colder-than-present climate in MH, and the use of the present fixed-length calendar causes a cooling bias (within -0.5 K) for the Northern Hemisphere and Antarctic, as well as a warming bias (within 0.3 K) for the Southern Hemisphere oceans. In boreal summer, the key characteristic shared in both angular and classical means is a warming over the Arctic Ocean, North Atlantic and Eurasia, led by increased JJA insolation in MH as compared to PI. Such warming is more pronounced in angular calendar than in classical calendar.

In LIG, the largest calendar effects on precipitation can be observed for SON over the tropical rain-belt (Fig. 5), with positive anomalies (within 30 mm/month) to the north and negative anomalies (up to -30 mm/month) to the south of the Inter Tropical Convergence Zone (ITCZ). Similar pattern can be seen for DJF, though with less pronounced magnitudes. For JJA the adjusted-minus-unadjusted precipitation anomalies present a dryness (up to -15 mm/month) and wetness (less than 10 mm/month) over the northern and southern edge of the ITCZ, respectively, opposite to the patterns for SON and DJF. The calendar effect appears to be small during boreal spring, as the vernal equinox is fixed at 21 March in both calendars. In contrast to the calendar-induced significant changes in large-scale patterns of LIG precipitation, the effect of calendar on MH precipitation is much less pronounced, showing positive (negative) anomalies up to 5 (-5) mm/month over the north (south) branch of the tropical rain-belt for all seasons. This is associated with the di-pole pattern of temperature differences between angular and classical means (warming over Northern Hemisphere and cooling over Southern Hemisphere). For PI, a northward displacement of ITCZ is obvious during SON for angular mean as compared to classical mean precipitation. While, for other seasons, no pronounced changes in precipitation can be observed.

The anomalies in precipitation (LIG-PI), as well as the impact of calendar conversion on the precipitation anomalies are shown in Fig. 6. The general patterns of precipitation anomalies (LIG-PI) are very similar for both angular and classical means, revealing a northward shift of the ITCZ especially from JJA through SON, evidenced in the wetter condition to the north of ITCZ and the drier condition to the south. Such pattern is overestimated in JJA and underestimated in SON when the present fixed-length calendar is applied. For both calendars, MH also presents a similar distribution in precipitation anomalies as for LIG, with a much smaller magnitude. Moreover, the application of the classical calendar leads to an underestimation of the increased summer monsoon rainfall in MH as compared to PI over the Northern Hemisphere monsoon domains, i.e., West Africa, North America, and South Asia.

Overall, it is crucial to perform calendar conversion before examining the surface temperature and precipitation differences between LIG/MH and PI, as non-ignorable artificial bias can be introduced to the seasonal cycle of temperature and precipitation with the application of present fixed-length calendar, which could be misinterpreted as climatic feedbacks.

Daily output takes up much more space than monthly output, so most model groups only provide monthly frequency variables. Here, we utilize a calendar transformation method that requires only the raw (i.e., classical "fixed-length" calendar) monthly mean values (Rymes and Myers, 2001). Using this approach, we perform calendar corrections based on the monthly outputs of the same 9 model groups. We then check the deviation of this month-length adjusted values from the day-length

https://doi.org/10.5194/cp-2021-163
Preprint. Discussion started: 29 November 2021


Climate of the Past Discussions

adjusted values. From Fig. S6 and Fig. S7 we can conclude that the conversion of calendar based on monthly mean values can improve the seasonal cycle to a large degree. For MH and PI, we observe only slight bias, with the temperature deviation being less than ± 0.05 K and precipitation deviation less than ± 1 mm/month, indicating that the calendar transformation based on monthly data can serve as an alternative for seasonal adjustment of MH and PI. However for LIG there are still significant warming bias over the high-latitude continents in JJA. During boreal autumn, the land is generally cooler and the tropics and Southern Ocean are generally warmer compared to the day-length adjusted values.

As stated above, we find spatial heterogeneity in the response of surface air temperature to calendar conversion across the globe, which is manifested in the opposite signals between two hemispheres and the contrast between land and ocean. Our model ensemble shows that the calendar effect is more pronounced over continents than over seawater areas. Here we calculate the seasonal cycle of surface air temperature for: (1) the original daily average, (2) the original monthly average, (3) daily length-adjusted mean values, and (4) month-length adjusted mean values, over different continents, shown in Fig. 8. We find the day-length and month-length adjusted values are very similar, evidenced in the overlapping orange and purple solid lines in Fig. 8. This suggests that the monthly calendar correction approach can serve as a good alternative when only monthly frequency model outputs are available for surface air temperature. For North America and Eurasia, we observe a slight positive anomaly in the PI between adjusted and unadjusted surface temperatures from January to July (less than 0.2 K), while negative anomalies are found from August to December, with the maximum change occurring in October (-0.7 K). For the Antarctic, the greatest calendar effect occurs in October and November, with the mean adjusted-minus-unadjusted value being 0.8 K. This agrees with the spatial maps shown in Fig. S5. For the MH, the calendar effect over North America and Eurasia appears to be greatest in May-June (0.5 K) and October-December (0.6 K). Over the Antarctic continent, apart from the warming in January-February (0.5 K) and the cooling in November (-0.7 K), no significant response of the mean surface air temperature to the calendar conversion was found. In terms of the LIG, the mean adjusted-minus-unadjusted surface air temperature in October reached up to 3 K in both North America and Eurasia. The maximum temperature change in Antarctica also occurs in October, with a magnitude of -3 K. In addition, we calculated the seasonal cycle of precipitation values for the following monsoon domains: North America (5-30°N, 120-40°W), African monsoon region (5-23.3°N, 15W-30°E), and South Asia (5-23.3°N, 70°W-120°E). As shown in Fig. 9, again we see very similar day-length and month-length adjusted values. Therefore, performing calendar correction based on monthly precipitation can help reduce the artificial distortion of monsoon rains to a large extent.

3.4 Calendar effects in transient simulations

Calendar effects should be considered also in the analysis of transient simulations (Bartlein and Shafer, 2019). Here with the utility of 3 mid-Holocene-to-present transient runs based on AWI-ESM, MPI-ESM and IPSL respectively, we examine the degree of influence of calendar definition on surface air temperature and precipitation. All the three experiments provide outputs in monthly frequency, therefore we perform calendar transformation based on monthly surface air temperature and precipitation using the approach described by Rymes and Myers (2001).

https://doi.org/10.5194/cp-2021-163
Preprint. Discussion started: 29 November 2021

The time series plotted in Fig. 10 are for adjusted and unadjusted mean surface air temperature over the Northern Hemisphere ice-free continents (i.e., North America, Eurasia, and northern Africa) for all seasons. Based on all the 3 models, the largest deviation between angular and classical mean temperature values happens in boreal autumn between 6 and 4.4 ka, with the temperature being underestimated under the present "fixed-length" calendar. Another distinct difference between month-length adjusted and unadjusted values occurs in boreal autumn between 4.4 and 0 ka. During this time interval, the surface air temperature over Northern Hemisphere ice-free continents can be overestimated with the use of the classical calendar. This phenomenon, again, highlights the importance of calendar correction in the analysis of both mid-Holocene and pre-industrial climates, especially in boreal autumn. Without the calculation of angular seasonality, the warming in the mid-Holocene relative to pre-industrial in SON can be largely underestimated. In DJF, no obvious deviation is found between the angular and classical means, evidenced in the overlapped black and red lines in the top panels of Fig. 10. During boreal spring, all the 3 models reveal a slight cooling bias in the original temperature values throughout the whole integrated time period, which is relatively more manifested in the mid-Holocene than in the late-Holocene and pre-industrial. In JJA, we observe a model-dependency of the calendar effects. AWI-ESM reveals a slight cooling bias and warming bias in the original JJA-mean surface air temperature for 6-3 ka and 3-0 ka respectively. In the transient run by MPI-ESM, the Northern Hemisphere temperature in JJA is underestimated under the classical calendar for the time period of 6-3 ka, consistent with the results of AWI-ESM. But no clear difference between adjusted and unadjusted values occurs after 3 ka in MPI-ESM. While in the IPSL simulation, it is shown that a slight cooling bias in the classical temperature values happens from 6 to 0 ka.

For the Southern Hemisphere ice-free lands (i.e., South America, Australia, and southern Africa), as shown in Fig. 11, the calendar effects are less pronounced as compared to Northern Hemisphere. Similar to the Northern Hemisphere, no distinct temperature deviation is seen for DJF. Besides, all the three models agree on the cooling bias in classical-mean temperatures in JJA (6-0 ka) and SON (4-0 ka), as well as a slight warming deviation during MAM (6-0 ka).

Fig. 12 illustrated the calendar effects on the Africa monsoon precipitation. The time series in Fig. 12 are derived by averaging month-length adjusted and unadjusted boreal summer precipitation over the land points within 5-23.3°N, 15W-30°E. All the 3 transient simulations show an artificial drying bias in the Africa monsoon precipitation with the application of the "fixed-length" calendar in 6 ka. It is also shown that, such calendar effect gradually becomes weaker from mid-Holocene to present.

4 Discussion and conclusions

Two important elements should be taken into consideration when comparing different paleoclimate simulations: the phasing of the insolation curve and the reference date. Artificial bias emerges when precessional effects are ignored, and such bias can be amplified by eccentricity changes (Joussaume and Braconnot, 1997). To avoid such bias, one shall define the seasonal cycle based on astronomical positions along the elliptical orbits. The sensitivity of simulated paleoclimate conditions to the "classical" and "angular" calendars had been investigated in a former study based on one single coarse resolution model (Joussaume and Braconnot, 1997), in which the authors state that the differences between the two calendar means cannot be

https://doi.org/10.5194/cp-2021-163
Preprint. Discussion started: 29 November 2021


Climate of the Past Discussions
Open Access
EGU

neglected. Here by examining 7 of the most advanced climate models in PMIP4, we again confirm the necessity of calendar definition in paleoclimate modelling research.

In the present paper, we use March 21st as the reference VE date, and perform calendar correction for 3 climatic periods: the pre-industrial, the mid-Holocene, and the Last interglacial. The results indicate that the precessional effects are the strongest in the Last interglacial, with the strongest effect for boreal autumn. In autumn, the classical mean Northern Hemisphere temperature in Last interglacial has a severe cooling bias, which largely impacts the anomaly between Last interglacial and pre-industrial. Similar case is also found for mid-Holocene, just with a less pronounced magnitude. It should be pointed out that, even though today's season lengths are in phase with the orbital definition of seasons, today's calendar is not an angular calendar. To be consistent, today's calendar also needs to be corrected, and this leads to non-ignorable changes in autumn.

Performing calendar conversion on daily data can completely erase the temperature and precipitation bias, however, due to the large volume of daily outputs, they are not preserved by most model groups. A mean preserving algorithm has been introduced (Rymes and Myers, 2001), with which the daily time series can be reconstructed. By performing calendar correction on the reconstructed daily time series, we find that the seasonal pattern in temperature and precipitation can be largely ameliorated, even though there is still room for improvement.

Another indication from the present paper is that the calendar definition can greatly affect the calculated Africa monsoon rainfall in the LIG, which starts from late June and ends in October (Zhang and Cook, 2014; Sultan and Janicot, 2003). We find that using a classical calendar leads to overestimation (underestimation) of Africa monsoon rainfall in boreal summer (autumn). Therefore, consideration of the calendar conversion is very essential for investigating the Africa monsoon precipitation.

The "pure" calendar effect was examined in an earlier study by implementing the paleo angular calendar into a modern climate state (Bartlein and Shafer, 2019) . Our results from model-ensemble equilibrium simulations show a good agreement with Bartlein and Shafer (2019) with regard to the calendar effect on the seasonality of surface air temperature and precipitation for the mid-Holocene and last interglacial. However, comparing results of our transient simulations with that from the TraCE-21ka transient simulation, as it was investigated in Bartlein and Shafer (2019), distinct differences emerge for the boreal autumn surface air temperature near present-day. As can be seen from our study, the onset of boreal autumn in the angular calendar is delayed by 3 days compared to the classical fixed-day calendar, resulting in negative anomalies in the adjusted-minus-unadjusted surface air temperature during SON. It should be noted that these discrepancies are not due to the different models used in our studies, but rather to the different approaches adopted for calendar conversion: In Bartlein and Shafer (2019), as well as in Joussaume and Braconnot (1997), it is assumed that the seasons defined by classical calendar very well match the phasing of insolation curves, therefore in their studies the angular seasons were calculated according to astronomical positions corresponding to the seasons in modern calendar. As a result of this assumption, there is no change in seasonality for the present-day in the studies of Bartlein and Shafer (2019) and Joussaume and Braconnot (1997).

An interesting phenomenon shared by our model-ensemble transient simulations and TraCE-21ka (Bartlein and Shafer, 2019) is that, around 6k all seasons show an increased surface air temperature over Northern Hemisphere continents in angular means compared to angular means (Fig. 10). The annual mean temperature should, however, be the same regardless of the seasonality definition used. This is due to the different lengths of seasons between the two approaches. Using the AWI-ESM

https://doi.org/10.5194/cp-2021-163
Preprint. Discussion started: 29 November 2021

Climate of the Past Discussions
Open Access
EGU

Table 3. The month-length weighted mean surface air temperature over Northern Hemisphere ice-free continents at 6k, as simulated by AWI-ESM. Units: °C.

Season	Angular mean	Classical mean	Anomaly (angular minus classical mean)
DJF	-6.25081	-6.9326	0.06971455
MAM	4.80496	4.56874	0.236228
JJA	19.478	19.4237	0.05435944
SON	6.35692	6.25081	0.1061139
Annual	5.89641	5.89641	0

6k as an example, in Table 3 we list the month-length weighted mean surface air temperature over the ice-free continents of the Northern Hemisphere in each season for both calendars. Despite a warming in all seasons, as shown in the last column of Table 3, there is no difference in the season-length weighted annual mean temperature for the angular calendar (Ta) and classical calendar (Tc), which are calculated as follows:

Ta = (Ta_djf*92+Ta_mam*94+Ta_jja*91+Ta_son*88)/365 = 5.89641

Tc = (Tc_djf*90+Tc_mam*92+Tc_jja*92+Tc_son*91)/365 = 5.89641

Therefore, our results support the strategy as described in Zhao et al. (2021): when averaging modeled variables across multiple months/seasons, it is desirable to perform calendar correction and to take into consideration the lengths of each month/season in order to avoid extra artificial bias introduced by the calculation, or directly use the daily output if available.

There are inconsistencies between proxy-based and modeled climate, for example, the temperature evolution from early to late Holocene has been shown to have a cooling and warming trend in observational reconstructions and transient simulations (Liu et al., 2014; Marcott et al., 2013), and the amplitude of the mid-to-late Holocene trends are largely underestimated in models compared to data (Lohmann et al., 2013). The underlying reason for the model-proxy inconsistency might rely on the uncertainties of both temperature reconstruction and model simulation (Lohmann et al., 2013; Liu et al., 2014; Pfeiffer and Lohmann, 2016). Since paleoclimate data often record the seasonal signal (e.g. local summer), a proper choice of the calendar is important for the temperature interpretation in models and data. A logical next step would be to perform the correction of the seasonal cycle in transient climate simulations covering the last glacial-interglacial cycle.

Data availability. The daily model outputs from the PMIP4 equilibrium simulations used in the present study can be downloaded from the Earth System Grid Federation (ESGF): https://esgf-data.dkrz.de/projects/esgf-dkrz/. The data from the transient simulations can be accessed by contacting XS (AWI-ESM), RD (MPI-ESM), and PB (IPSL).

Author contributions. XS, GL and EI developed the original idea for this study. XS conducted the AWI-ESM experiments, produces all figures and wrote the initial draft under the supervision of MW and GL. CK wrote the scripts for calendar correction, and drafted the

https://doi.org/10.5194/cp-2021-163
Preprint. Discussion started: 29 November 2021

methodology section. EI performed calendar correction and first analysis under the supervision of XS and GL. CK, CB, AZ, PB and XL gave very constructive comments and suggestions. DS provided technical help of AWI-ESM. RD and JJ performed MPI-ESM transient simulation. PB performed IPSL transient simulation. EB, JC, BO, RT, EV, HY, QZ and WZ performed key PMIP4 equilibrium experiments and contributed their respective model outputs.

Competing interests. The authors have declared that no competing interests exist.

Acknowledgements. The present study is supported by Alfred Wegener Institute, Helmholtz center for Polar and Marine Research; the PAlaeo-Constraints on Monsoon Evolution and Dynamics (PACMEDY) Belmont Forum project; German Federal Ministry of Education and Science (BMBF) PalMod II WP 3.3 (grant no. 01LP1924B); The AWI-ESM simulations were conducted on Deutsche Klimarechenzentrum (DKRZ) and AWI supercomputer (Ollie). XL is funded by the open fund of State Key Laboratory of Loess and Quaternary Geology, Institute of Earth Environment, CAS (grant no. SKLLQG1920) and the National Science Foundation for Young Scientists of China (grant no. 41807425); RD is funded by the Deutsche Forschungsgemeinschaft (DFG, German Research Foundation) under Germany's Excellence Strategy – EXC 2037 Climate, Climatic Change, and Society (CLICCS) - Cluster of Excellence Hamburg, A4 African and Asian Monsoon Margins – Project Number: 390683824; QZ is funded by the Swedish Research Council (Vetenskapsrdet, grant no. 2013-06476 and 2017-04232). The EC-Earth simulations were performed on HPC resources provided by the Swedish National Infrastructure for Computing (SNIC) at the National Supercomputer Centre (NSC).

https://doi.org/10.5194/cp-2021-163
Preprint. Discussion started: 29 November 2021

Climate of the Past Discussions
Open Access
EGU

References

Bader, J., Jungclaus, J., Krivova, N., Lorenz, S., Maycock, A., Raddatz, T., Schmidt, H., Toohey, M., Wu, C.-J., and Claussen, M.: Global temperature modes shed light on the Holocene temperature conundrum, Nature Communications, 11, 1–8, 2020.

Bartlein, P. J. and Shafer, S. L.: Paleo calendar-effect adjustments in time-slice and transient climate-model simulations (PaleoCalAdjust v1. 0): Impact and strategies for data analysis, Geoscientific Model Development, 12, 3889–3913, 2019.

Berger, A.: Long-term variations of the earth's orbital elements, Celestial Mechanics, 15, 53–74, 1977.

Braconnot, P., Otto-Bliesner, B., Harrison, S., Joussaume, S., Peterchmitt, J.-Y., Abe-Ouchi, A., Crucifix, M., Driesschaert, E., Fichefet, T., Hewitt, C., et al.: Results of PMIP2 coupled simulations of the Mid-Holocene and Last Glacial Maximum–Part 2: feedbacks with emphasis on the location of the ITCZ and mid-and high latitudes heat budget, 2007.

Braconnot, P., Zhu, D., Marti, O., and Servonnat, J.: Strengths and challenges for transient Mid-to Late Holocene simulations with dynamical vegetation, Climate of the Past, 15, 997–1024, 2019.

Brierley, C. M., Zhao, A., Harrison, S. P., Braconnot, P., Williams, C. J., Thornalley, D. J., Shi, X., Peterschmitt, J.-Y., Ohgaito, R., Kaufman, D. S., et al.: Large-scale features and evaluation of the PMIP4-CMIP6 midHolocene simulations, Climate of the Past, 16, 1847–1872, 2020.

Brovkin, V., Lorenz, S., Raddatz, T., Ilyina, T., Stemmler, I., Toohey, M., and Claussen, M.: What was the source of the atmospheric CO 2 increase during the Holocene?, Biogeosciences, 16, 2543–2555, 2019.

Cao, J., Wang, B., Young-Min, Y., Ma, L., Li, J., Sun, B., Bao, Y., He, J., Zhou, X., and Wu, L.: The NUIST Earth System Model (NESM) version 3: description and preliminary evaluation, Geoscientific Model Development, 11, 2975–2993, 2018.

Danby, J. and Burkardt, T.: The solution of Kepler's equation, I, Celestial Mechanics, 31, 95–107, 1983.

Fischer, N. and Jungclaus, J.: Effects of orbital forcing on atmosphere and ocean heat transports in Holocene and Eemian climate simulations with a comprehensive Earth system model, Climate of the Past, 6, 155–168, 2010.

Gettelman, A., Hannay, C., Bacmeister, J., Neale, R., Pendergrass, A., Danabasoglu, G., Lamarque, J.-F., Fasullo, J., Bailey, D., Lawrence, D., et al.: High climate sensitivity in the Community Earth System Model Version 2 (CESM2), Geophysical Research Letters, 46, 8329–8337, 2019.

He, B., Bao, Q., Wang, X., Zhou, L., Wu, X., Liu, Y., Wu, G., Chen, K., He, S., Hu, W., et al.: CAS FGOALS-f3-L Model Datasets for CMIP6 Historical Atmospheric Model Intercomparison Project Simulation, Advances in Atmospheric Sciences, 36, 771–778, 2019.

Jiang, D., Tian, Z., and Lang, X.: Mid-Holocene global monsoon area and precipitation from PMIP simulations, Climate Dynamics, 44, 2493–2512, 2015.

Joos, F. and Spahni, R.: Rates of change in natural and anthropogenic radiative forcing over the past 20,000 years, Proceedings of the National Academy of Sciences, 105, 1425–1430, 2008.

Joussaume, S. and Braconnot, P.: Sensitivity of paleoclimate simulation results to season definitions, Journal of Geophysical Research: Atmospheres, 102, 1943–1956, 1997.

Kageyama, M., Braconnot, P., Harrison, S. P., Haywood, A. M., Jungclaus, J. H., Otto-Bliesner, B. L., Peterschmitt, J.-Y., Abe-Ouchi, A., Albani, S., Bartlein, P. J., et al.: The PMIP4 contribution to CMIP6–Part 1: Overview and over-arching analysis plan, Geoscientific Model Development, 11, 1033–1057, 2018.

https://doi.org/10.5194/cp-2021-163
Preprint. Discussion started: 29 November 2021

Kageyama, M., Harrison, S. P., Kapsch, M.-L., Lofverstrom, M., Lora, J. M., Mikolajewicz, U., Sherriff-Tadano, S., Vadsaria, T., Abe-Ouchi, A., Bouttes, N., et al.: The PMIP4 Last Glacial Maximum experiments: preliminary results and comparison with the PMIP3 simulations, Climate of the Past, 17, 1065–1089, 2021a.

Kageyama, M., Sime, L. C., Sicard, M., Guarino, M.-V., de Vernal, A., Stein, R., Schroeder, D., Malmierca-Vallet, I., Abe-Ouchi, A., Bitz, C., et al.: A multi-model CMIP6-PMIP4 study of Arctic sea ice at 127 ka: sea ice data compilation and model differences, Climate of the Past, 17, 37–62, 2021b.

Köhler, P., Nehrbass-Ahles, C., Schmitt, J., Stocker, T. F., and Fischer, H.: A 156 kyr smoothed history of the atmospheric greenhouse gases CO 2, CH 4, and N 2 O and their radiative forcing, Earth System Science Data, 9, 363–387, 2017.

Kukla, G. J., Bender, M. L., de Beaulieu, J.-L., Bond, G., Broecker, W. S., Cleveringa, P., Gavin, J. E., Herbert, T. D., Imbrie, J., Jouzel, J., et al.: Last interglacial climates, Quaternary Research, 58, 2–13, 2002.

Li, L., Yu, Y., Tang, Y., Lin, P., Xie, J., Song, M., Dong, L., Zhou, T., Liu, L., Wang, L., et al.: The flexible global ocean-atmosphere-land system model grid-point version 3 (fgoals-g3): description and evaluation, Journal of Advances in Modeling Earth Systems, 12, e2019MS002 012, 2020.

Liu, Z., Zhu, J., Rosenthal, Y., Zhang, X., Otto-Bliesner, B. L., Timmermann, A., Smith, R. S., Lohmann, G., Zheng, W., and Timm, O. E.: The Holocene temperature conundrum, Proceedings of the National Academy of Sciences, 111, E3501–E3505, 2014.

Lohmann, G., Pfeiffer, M., Laepple, T., Leduc, G., and Kim, J.-H.: A model-data comparison of the Holocene global sea surface temperature evolution, Climate of the Past, pp. 1807–1839, 2013.

Lunt, D., Abe-Ouchi, A., Bakker, P., Berger, A., Braconnot, P., Charbit, S., Fischer, N., Herold, N., Jungclaus, J. H., Khon, V., et al.: A multi-model assessment of last interglacial temperatures, Climate of the Past, 9, 699–717, 2013.

Lurton, T., Balkanski, Y., Bastrikov, V., Bekki, S., Bopp, L., Braconnot, P., Brockmann, P., Cadule, P., Contoux, C., Cozic, A., et al.: Implementation of the CMIP6 forcing data in the IPSL-CM6A-LR model, Journal of Advances in Modeling Earth Systems, 2020.

Marcott, S. A., Shakun, J. D., Clark, P. U., and Mix, A. C.: A reconstruction of regional and global temperature for the past 11,300 years, science, 339, 1198–1201, 2013.

Nikolova, I., Yin, Q., Berger, A., Singh, U., and Karami, M.: The last interglacial (Eemian) climate simulated by LOVECLIM and CCSM3., Climate of the Past Discussions, 8, 2012.

Otto-Bliesner, B., Braconnot, P., Harrison, S., Lunt, D., Abe-Ouchi, A., Albani, S., Bartlein, P., Capron, E., Carlson, A., Dutton, A., et al.: The PMIP4 contribution to CMIP6–Part 2: Two interglacials, scientific objective and experimental design for Holocene and Last Interglacial simulations, 2017.

Otto-Bliesner, B. L., Brady, E. C., Zhao, A., Brierley, C. M., Axford, Y., Capron, E., Govin, A., Hoffman, J. S., Isaacs, E., Kageyama, M., et al.: Large-scale features of Last Interglacial climate: results from evaluating the lig127k simulations for the Coupled Model Intercomparison Project (CMIP6)–Paleoclimate Modeling Intercomparison Project (PMIP4), Climate of the Past, 17, 63–94, 2021.

Pfeiffer, M. and Lohmann, G.: Greenland Ice Sheet influence on Last Interglacial climate: global sensitivity studies performed with an atmosphere–ocean general circulation model, Climate of the Past, pp. 1313–1338, 2016.

Rackow, T., Goessling, H. F., Jung, T., Sidorenko, D., Semmler, T., Barbi, D., and Handorf, D.: Towards multi-resolution global climate modeling with ECHAM6-FESOM. Part II: climate variability, Climate dynamics, 50, 2369–2394, 2018.

Rymes, M. and Myers, D.: Mean preserving algorithm for smoothly interpolating averaged data, Solar Energy, 71, 225–231, 2001.

Shi, X. and Lohmann, G.: Simulated response of the mid-Holocene Atlantic meridional overturning circulation in ECHAM6-FESOM/MPIOM, Journal of Geophysical Research: Oceans, 121, 6444–6469, 2016.

https://doi.org/10.5194/cp-2021-163
Preprint. Discussion started: 29 November 2021

Shi, X., Lohmann, G., Sidorenko, D., and Yang, H.: Early-Holocene simulations using different forcings and resolutions in AWI-ESM, The Holocene, 30, 996–1015, 2020.

Sidorenko, D., Rackow, T., Jung, T., Semmler, T., Barbi, D., Danilov, S., Dethloff, K., Dorn, W., Fieg, K., Gößling, H. F., et al.: Towards multi-resolution global climate modeling with ECHAM6–FESOM. Part I: model formulation and mean climate, Climate Dynamics, 44, 757–780, 2015.

Sidorenko, D., Goessling, H., Koldunov, N., Scholz, P., Danilov, S., Barbi, D., Cabos, W., Gurses, O., Harig, S., Hinrichs, C., et al.: Evaluation of FESOM2. 0 coupled to ECHAM6. 3: preindustrial and HighResMIP simulations, Journal of Advances in Modeling Earth Systems, 11, 3794–3815, 2019.

Sultan, B. and Janicot, S.: The West African monsoon dynamics. Part II: The "preonset" and "onset" of the summer monsoon, Journal of climate, 16, 3407–3427, 2003.

Volodin, E. M., Mortikov, E. V., Kostrykin, S. V., Galin, V. Y., Lykossov, V. N., Gritsun, A. S., Diansky, N. A., Gusev, A. V., Iakovlev, N. G., Shestakova, A. A., et al.: Simulation of the modern climate using the INM-CM48 climate model, Russian Journal of Numerical Analysis and Mathematical Modelling, 33, 367–374, 2018.

Zhang, G. and Cook, K. H.: West African monsoon demise: Climatology, interannual variations, and relationship to seasonal rainfall, Journal of Geophysical Research: Atmospheres, 119, 10–175, 2014.

Zhang, Q., Berntell, E., Axelsson, J., Chen, J., Han, Z., de Nooijer, W., Lu, Z., Li, Q., Zhang, Q., Wyser, K., et al.: Simulating the mid-Holocene, last interglacial and mid-Pliocene climate with EC-Earth3-LR, Geoscientific Model Development, 14, 1147–1169, 2021.

Zhao, A., Brierley, C. M., Jiang, Z., Eyles, R., Oyarzún, D., and Gomez-Dans, J.: Analyzing the PMIP4-CMIP6 ensemble: a workflow and tool (pmip_p2fvar_analyzer v1), Geoscientific Model Development Discussions, pp. 1–22, 2021.

https://doi.org/10.5194/cp-2021-163
Preprint. Discussion started: 29 November 2021

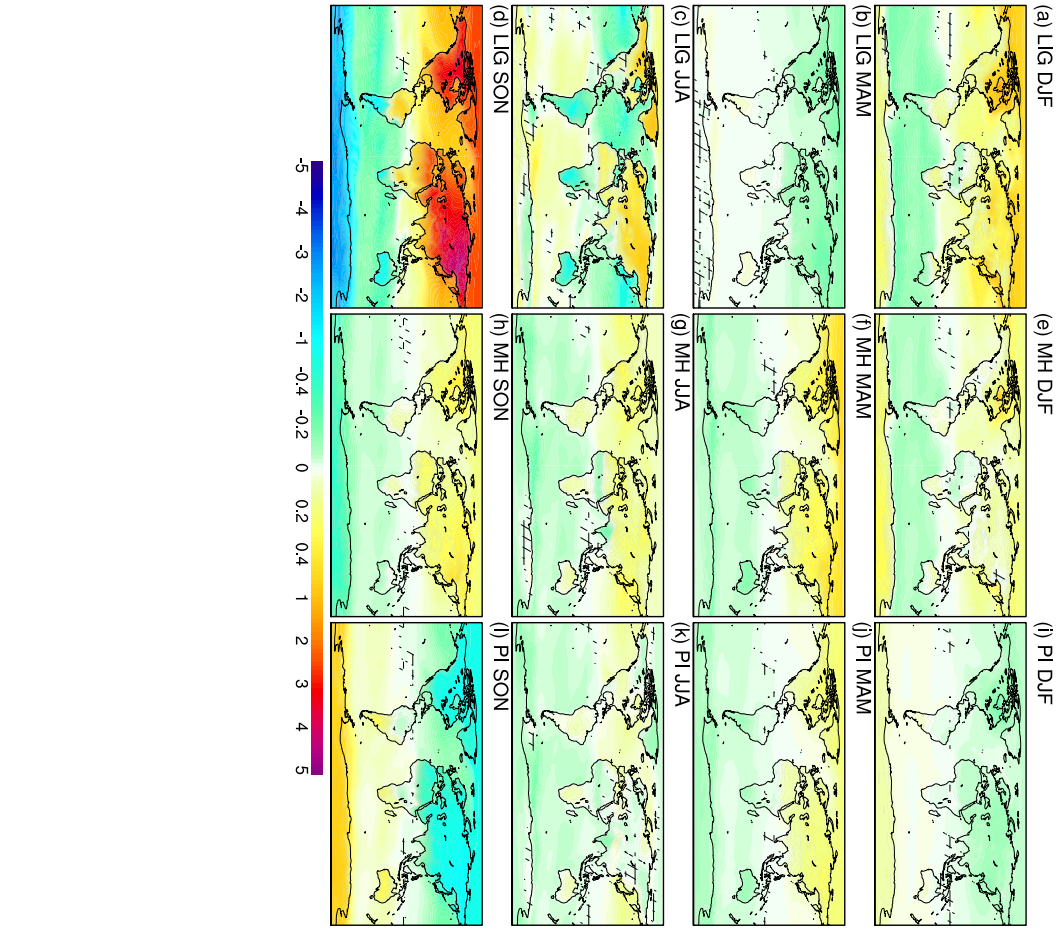

Figure 1. Anomalies of surface air temperature between angular means and classical means. The unmarked area indicates that at least 7 out of the 9 models show the same sign. Units: K.

https://doi.org/10.5194/cp-2021-163
Preprint. Discussion started: 29 November 2021

Climate of the Past Discussions
Open Access
EGU

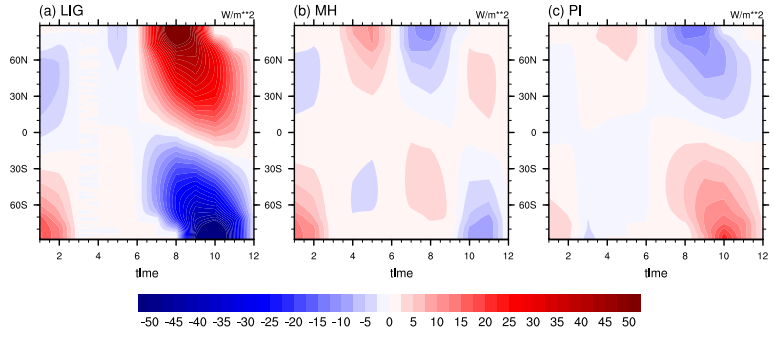

Figure 2. Insolation anomalies between angular and classical calendar for (a) LIG, (b) MH, and (c) PI.

https://doi.org/10.5194/cp-2021-163
Preprint. Discussion started: 29 November 2021

Climate of the Past
Discussions
Open Access
EGU

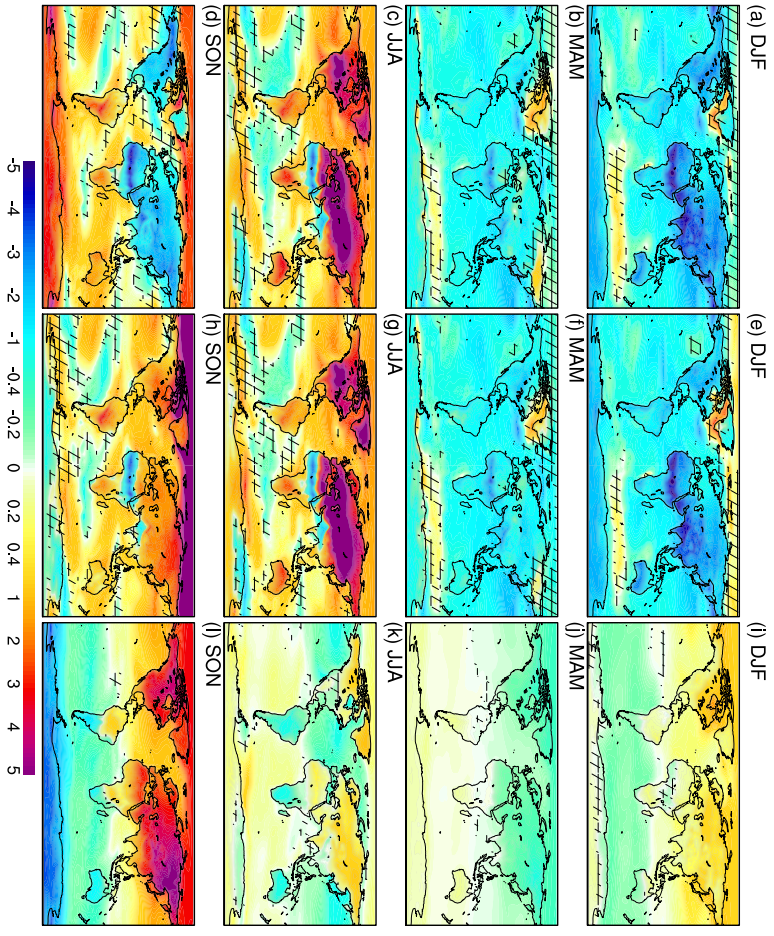

Figure 3. Surface air temperature for (a-d) LIG minus PI classical means, (e-h) LIG minus PI angular means, and (i-l) anomalies between LIG minus PI classical means and LIG minus PI angular means. The unmarked area indicates that at least 7 out of the 9 models show the same sign. Units: K.

https://doi.org/10.5194/cp-2021-163
Preprint. Discussion started: 29 November 2021

Climate of the Past Discussions

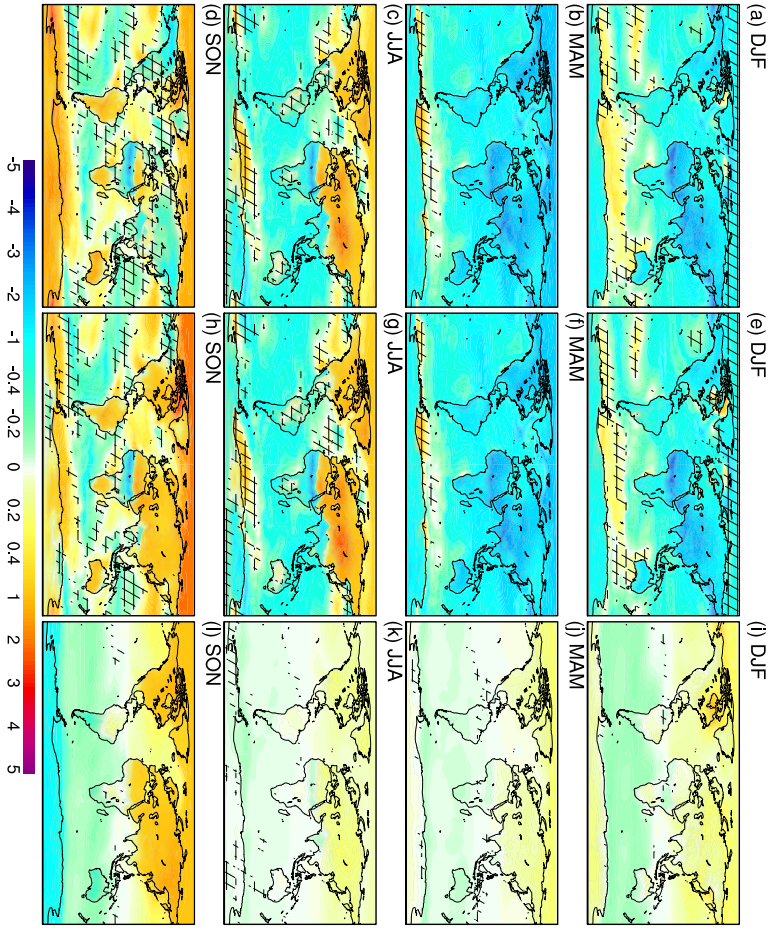

Figure 4. As Fig. 3, but for the MH.

https://doi.org/10.5194/cp-2021-163
Preprint. Discussion started: 29 November 2021

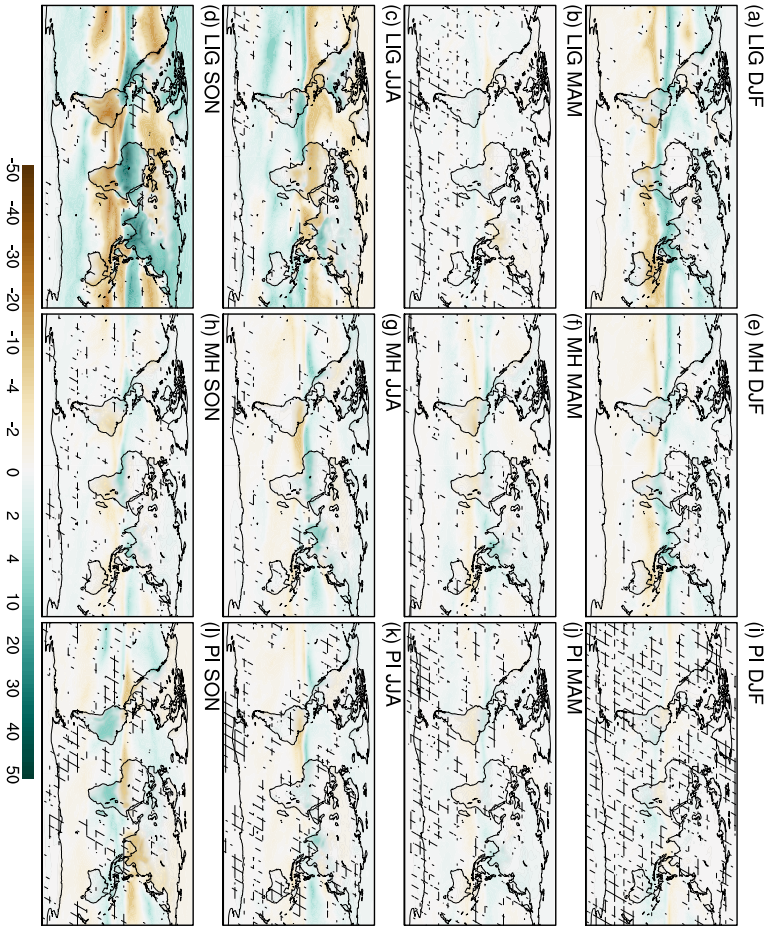

Figure 5. Anomalies of precipitation between angular means and classical means for (a-d) LIG, (e-h) MH, and (i-l) PI. The unmarked area indicates that at least 7 out of the 9 models show the same sign. Units: mm/month.

https://doi.org/10.5194/cp-2021-163
Preprint. Discussion started: 29 November 2021

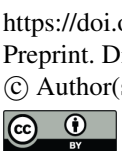

Climate of the Past Discussions
Open Access
EGU

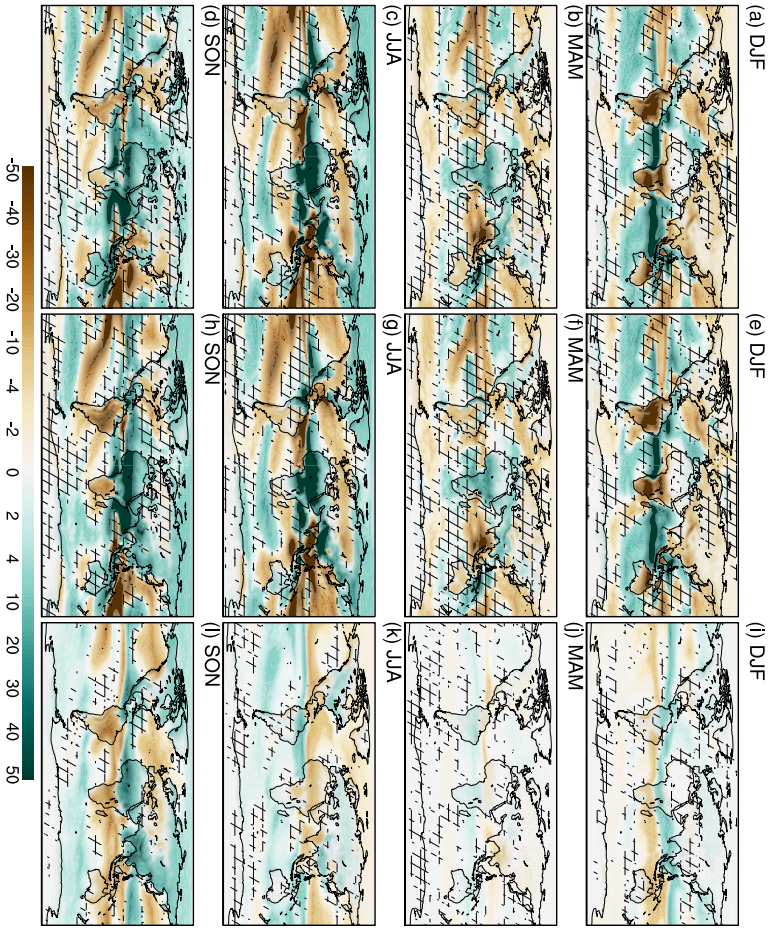

Figure 6. Precipitation for (a-d) LIG minus PI classical means, (e-h) LIG minus PI angular means, and (i-l) anomalies between LIG minus PI classical means and LIG minus PI angular means. The unmarked area indicates that at least 7 out of the 9 models show the same sign. Units: mm/month.

https://doi.org/10.5194/cp-2021-163
Preprint. Discussion started: 29 November 2021

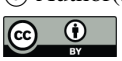

Climate of the Past Discussions

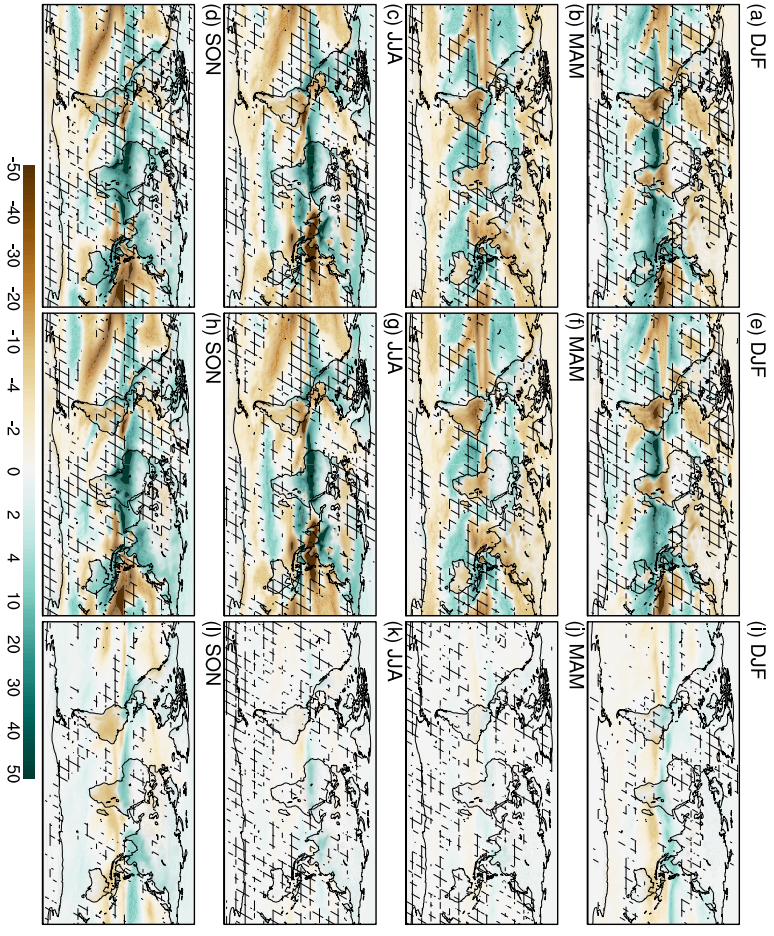

Figure 7. As Fig. 6, but for the MH.

https://doi.org/10.5194/cp-2021-163
Preprint. Discussion started: 29 November 2021

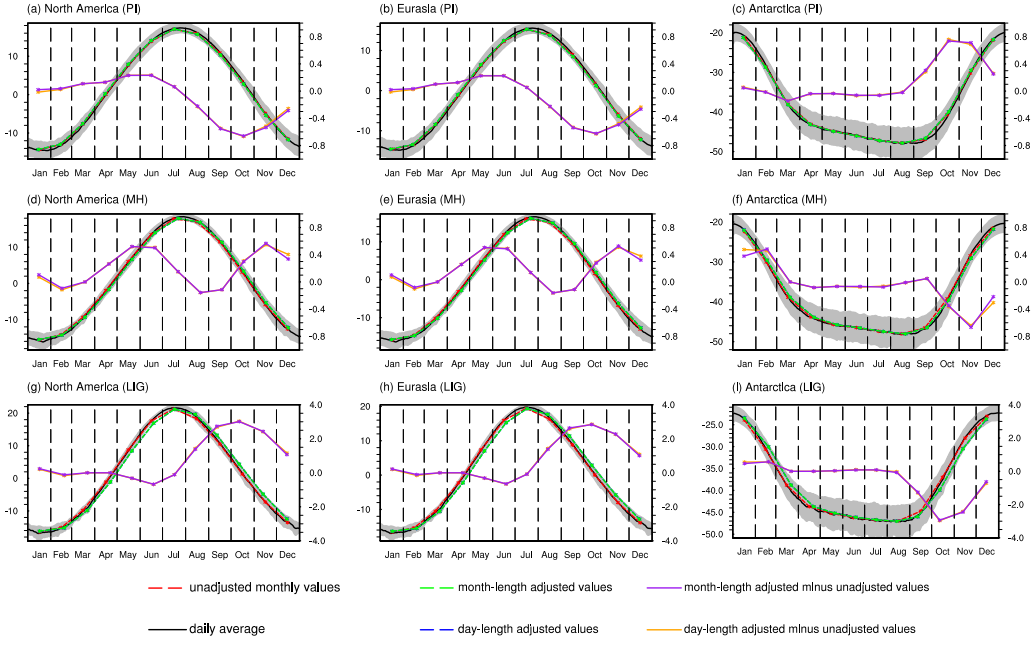

Figure 8. Seasonal cycle of regional mean surface air temperature in daily average (black solid lines), classical monthly means (red dashed lines), day-length adjusted means (blue dashed lines), and month-length adjusted means (green dashed lines) for (a-c) PI, (d-f) MH, and (g-i) LIG, axis to the left. Grey area represents one standard deviation from the multi-model ensemble daily mean values. Purple (orange) solid line represents the month-length (day-length) adjusted minus unadjusted values, axis to the right. The values are calculated by averaging the surface air temperatures over (a,d,g) North America, (b,e,h) Eurasia, and (c,f,i) Antarctica. Units: °C.

https://doi.org/10.5194/cp-2021-163
Preprint. Discussion started: 29 November 2021

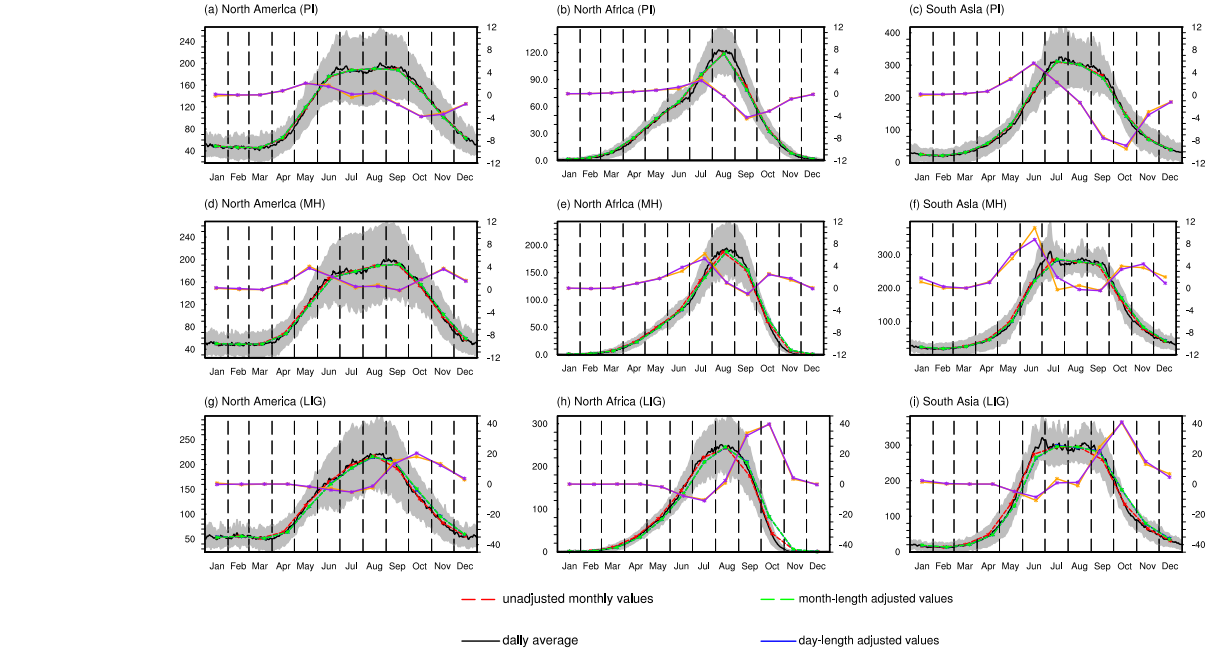

Figure 9. Seasonal cycle of regional mean precipitation in daily average (black solid lines), classical monthly means (red dashed lines), day-length adjusted means (blue dashed lines), and month-length adjusted means (green dashed lines) for (a-c) PI, (d-f) MH, and (g-i) LIG. Grey area represents one standard deviation from the multi-model ensemble daily mean values. Purple (orange) solid line represents the month-length (day-length) adjusted minus unadjusted values, axis to the right. The values are calculated by averaging the precipitation over (a,d,g) North America, (b,e,h) North Africa, and (c,f,i) South Asia. Units: mm/month.

https://doi.org/10.5194/cp-2021-163
Preprint. Discussion started: 29 November 2021

Climate of the Past Discussions
Open Access
EGU

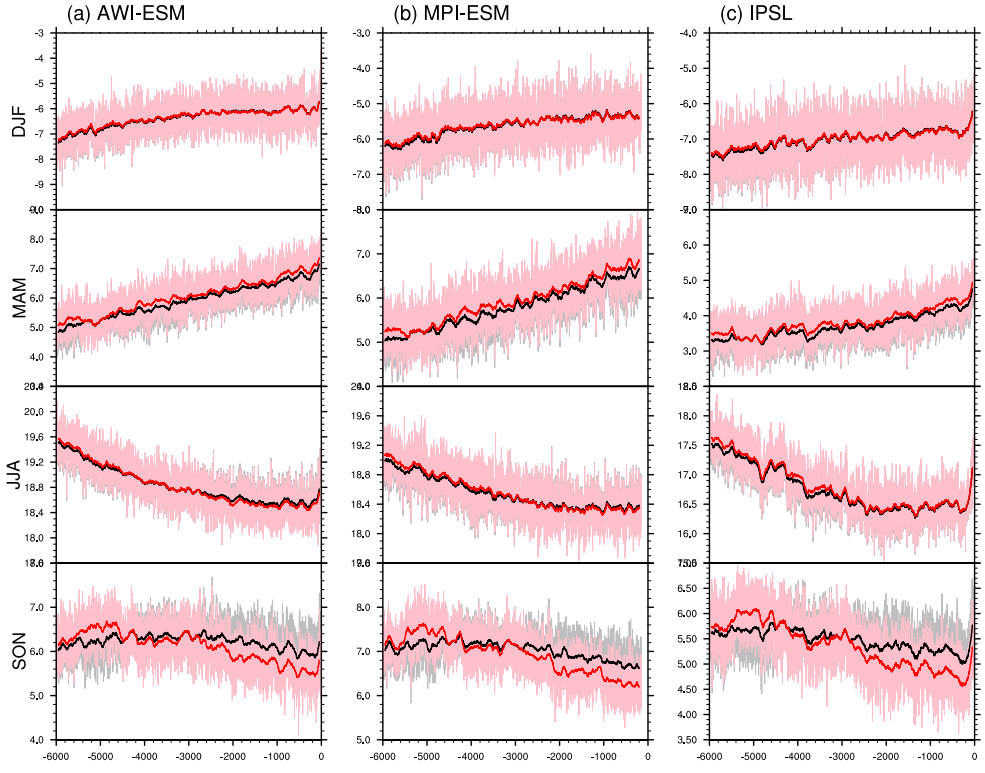

Figure 10. Time series of surface air temperature in classical and angular means averaged over Northern Hemisphere ice-free continents, weighted by month length, for (a) AWI-ESM, (b) MPI-ESM, and (c) IPSL. Grey and pink lines stand for the original classical and angular means respectively. Smoothed curves with a running window of 100 model years are shown in black (for classical means) and red (for angular means). Units: °C.

https://doi.org/10.5194/cp-2021-163
Preprint. Discussion started: 29 November 2021

Climate of the Past Discussions
Open Access
EGU

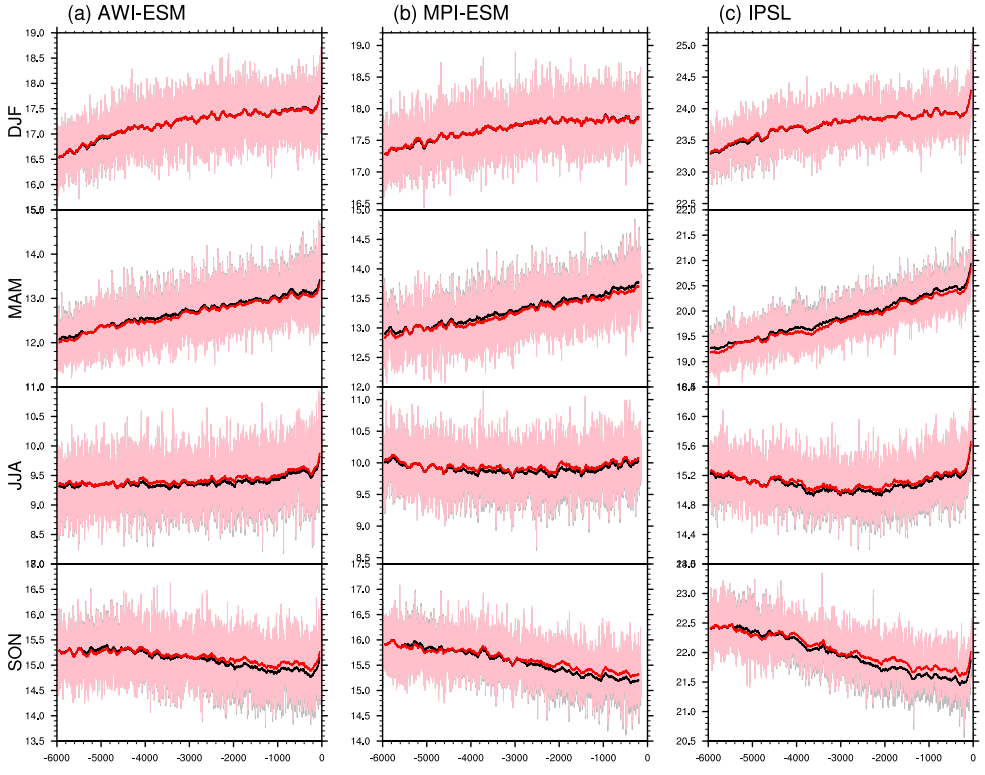

Figure 11. Time series of surface air temperature in classical and angular means averaged over Southern Hemisphere ice-free continents, weighted by month length, for (a) AWI-ESM, (b) MPI-ESM, and (c) IPSL. Grey and pink lines stand for the original classical and angular means respectively. Smoothed curves with a running window of 100 model years are shown in black (for classical means) and red (for angular means). Units: °C.

https://doi.org/10.5194/cp-2021-163
Preprint. Discussion started: 29 November 2021

Climate of the Past Discussions
Open Access
EGU

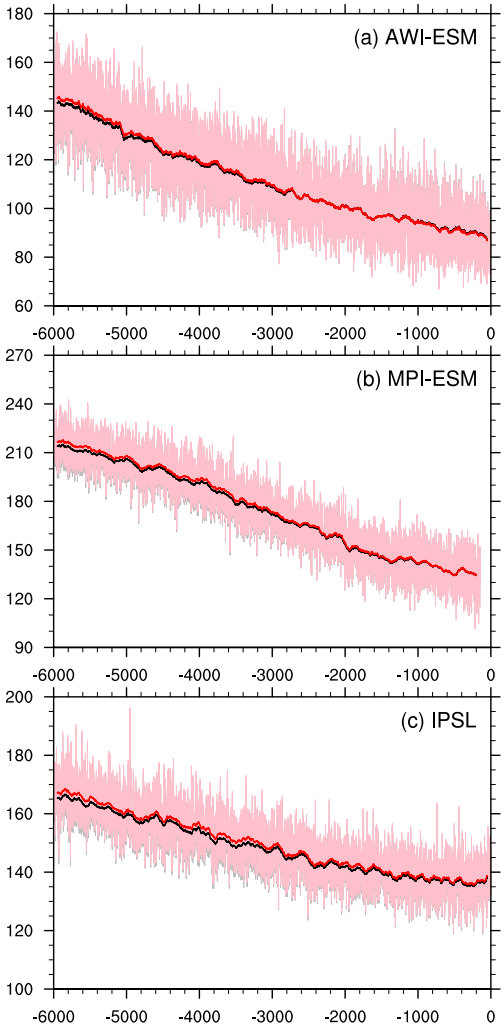

Figure 12. Time series of boreal summer precipitation in classical and angular means averaged over Africa monsoon zone (5-23.3°N, 15W-30°E), weighted by month length, for (a) AWI-ESM, (b) MPI-ESM, and (c) IPSL. Grey and pink lines stand for the original classical and angular means respectively. Smoothed curves with a running window of 100 model years are shown in black (for classical means) and red (for angular means). Units: mm/month.